RESEARCH ARTICLE

Immunohistochemical Staining for Nerve Fibers in Normal Tissues with Frozen Sections: Structure and Function Relationship

Tatsuo Tomita, M.D.

Department of Integrative Biosciences, Oregon Health and Science University, Portland, OR, USA

Email: tomitat39@gmail.com

ABSTRACT
Small nerve fibers are difficult to immunostain with routinely formalin-fixed and paraffin-embedded sections. Normal tissues except central nervous system are not densely innervated compared to densely distributed lymphatic and blood vessels and nerve fibers are not properly preserved in the routinely formalin-fixed and paraffin-embedded tissues. Nerve density technique with skin punch biopsy is an established method using 50 μm tissue sections, which are initially preserved in fixative. The fixed tissues are frozen sectioned and floating tissue sections are immunostained for nerve fiber markers. We had developed an alternative method using unfixed frozen sections mounted on glass slides. We had previously used this frozen section method for lymphatic and blood vessel immunohistochemistry and extended to nerve fiber immunostaining using neurofilament and CD56 as nerve fiber markers. Immunostained tissues with frozen sections were compared to formalin-fixed and paraffin-embedded colon and kidney sections. The normal tissues from rhesus monkey included heart, intestines, diaphragm, pancreas, spleen, kidney, thyroid, urinary bladder and others. Frozen section immunostained sections clearly depicted much more fine nerve fibers especially using CD56 as a nerve marker than with paraffin-embedded tissues. This technique is more labor-intensive but provides more precise distribution of fine nerve fibers than with routinely paraffin-embedded tissues. This immunostaining with frozen sections validated usefulness to depict more detailed nerve distribution and will shed light on normal histology and histopathology.
Keywords: CD56, frozen sections, immunohistochemistry, nerve fibers, neurofilament, normal rhesus monkey tissues

Introduction

With routinely formalin-fixed and paraffin-embedded tissues, specific immunohistochemical staining for nerve fiber is limited since nerve fiber antigens are expressed at low levels in the majority of normal organs except central nervous system[1]. Traditionally, Bielschowsky silver stain has been used to stain nerve fibers in degenerative brain diseases including Alzheimer's disease[2,3]. Nerve fibers are mixture of myelinated and unmyelinated nerves and peripheral nerve fibers are poorly stained in the routinely H & E sections, since individual axons are commonly small individual in dimeter (1 - 5μm) and myelin sheath of myelinated nerves are colorless in the H & E sections[1]. Thus, small nerve fibers are often indistinguishable from fibrotic fibers in the routinely formalin-fixed and paraffin-embedded sections[1]. The previously reported immunohistochemical studies of nerve fibers in the endometrium had been performed with routinely paraffin-embedded tissues[4-7]. Epidermal peripheral nerve fibers had been extensively studied with skin punch biopsy using 50 μm thick floating tissue sections[6-8] after being fixed in 2% paraformaldehyde and these procedures are very labor-intensive. Skin biopsy for the assessment of intradermal sensory nerve fiber using the pan-axonal marker, PGP 9.5 is an established clinical and research technique, and this technique may also be used to assess other population of nerve fibers in the other tissues[8-11]. We had previously utilized immunohistochemical staining with frozen sections for immunostaining lymphatic and blood vessels with normal monkey tissues[12,13] and extended this staining technique to immunostain peripheral nerve fibers in the normal tissues[14]. The current study aimed to detect the presence of nerve fibers in normal tissues including heart, lung, small intestine, large intestine, diaphragm, spleen, pancreas, adrenal gland, kidney, urinary bladder, vagina and normally cycling endometrium. The most commonly used marker for nerve fibers is PGP 9.5, which is a non-specific pan-axonal marker[15-17]. In this study we used antibodies against neurofilament (NF) and neural cell adhesion molecule, CAM (CD56). NF antibody is a highly specific immunohistochemical marker for myelinated nerve fibers, which immunostains Aβ, Adelta and B fibers, and Adelta fibers are small, myelinated fibers and transmit sharp, pricking localized pain to CNS[18-21]. C-fibers are small unmyelinated fibers and transmit dull, aching, burning poorly located pain[20,21]. CD56 expression is compatible to that of N-CAM and is expressed in thin nerve fibers, fine varicose and sensory nerve endings, cell membrane of ganglion cells, young, striated muscle cells, thick nerve fibers and perikaryal of ganglion cells while adult striated muscle fibers were reportedly CD56 negative[22-25]. Nitric oxide synthases (NOSs) are a family of enzymes catalyzing the production of nitric oxide from arginine[26]. Several cell types had been reported positive for NOS to be added as a marker for many neuroendocrine cells[20-24]. NOS has been added as a marker for nerve fibers and neuroendocrine cells[26,27].

Materials and Methods

Normal tissues of rhesus monkey were obtained at necropsy including heart, lung, small intestine, large intestine, diaphragm, spleen, pancreas, kidney, adrenal, thyroid, urinary bladder, vagina and cycling endometrium. The wedges of uterine tissue were processed from the cycling monkeys from Day 3 to Day 28. Additional monkeys were inserted with Silastic IUD (6 cm) into uterine cavity filled with an IUD containing progesterone antagonist, ZK 23011 (Leiras OY, Finland), which was kept for 5 months[28]. After the normal organs and uterus had been removed, a wedge of tissue from the inner endometrial surface to the myometrium including the full thickness of endometrium and contiguous myometrium was taken as described before at an average tissue size of 1 x 1 x 0.4 cm[12-14]. Fresh wedge tissues were microwave-irradiated for 7 sec in a microwave oven, embedded in OCT, frozen in liquid propane in the liquid nitrogen bath and frozen sectioned at 5 – 7 μm[12-14]. Frozen sections were mounted on Super Frost Plus slide (Fisher Scientific, Pittsburgh, PA), microwave-irradiated again on ice for 3 sec, fixed in 2% paraformaldehyde in phosphate buffer at pH 7.4 for 10 to15 min at room temperature, and immersed twice for 2 min each in 85% ethanol[12-14]. Sections were incubated with blocking serum for 20 min and then with monoclonal anti-human NF (clone 2F11) and monoclonal CD56 (Dako System, Carpenteria, CA) at 1:100 dilutions overnight at 4°C, respectively. The other sections of large intestine were also immunostained with rabbit anti-PGP 9.5 (Gene Tex, TGX 17039, Irvine, CA) and rabbit anti-NOS (SAB 45020111, Millipore Sigma, Burlington, MA) at 1 : 100 dilutions to compare immunostaining of nerve fibers with that of NF and CD56. After rinsing and immersion in blocking serum again, sections were incubated with second antibody (1 : 200 dilutions) for 30 min at room temperature. Final visualization was achieved with the ABC kit (Vector Laboratories, Burlinga-me, CA) using diaminobenzidine tetrahydrochloride (Dojindo Molecular Technology, Rockville, MD) for brown coloring. Tissue sections were then lightly counterstained with hematoxylin to facilitate identification of cellular components. Additional intestinal and kidney tissues were fixed in a mixture of 2% paraformaldehyde and 1% formalin and were

embedded in paraffin. The paraffin sections were treated for antigen retrieval procedure, then the sections were stained with rabbit-anti-PGP 9.5 and rabbit anti-NOS at 1: 100m dilutions for nerve fibers, respectively.

Results

Heart has rich myelinated and non-myelinated nerve fibers in the subepicardial connective tissue (Fig. 1-A) and a few infiltrating nerve fibers in the arterial wall of the ventricle by NF staining while CD56 immunostaining revealed more peri-arterial nerve fibers than NF immunostaining (Fig. 1-A and -B). In lung, a very few scattered non-myelinated nerve fibers were immunostained in the peri-arterial tissue equally by both NF and CD56 immunostaining (Fig.1-C and -D). In the cross sections of diaphragm, there were abundant plexuses and myelinated nerve fibers in the fibrous stroma, from which myelinated and non-myelinated fibers infiltrated into each muscle bundles by NF immunostaining and less non-myelinated nerve fibers by CD56 immunostaining (Fig. 1-E and -F). Duodenum had abundant nerve plexuses and myelinated nerve fibers in the deep submucosa (Meissner's plexus) and other myenteric plexuses between the inner and outer muscular layer (Auerbach's plexus) by NF staining (Fig. 2-A). CD 56 immunostaining revealed similar findings albeit less darker staining for intramuscular nerve bundled than NF staining (Fig. 2-B). Frozen sectioning large intestine was difficult and frozen sections were compared to the routinely paraffin-embedded sections. Frozen sections revealed multiple myelinated nerve bundles in the inner and outer smooth muscle layer with some vertically infiltrating non-myelinated nerve fibers in the inner circular muscle by NF immunostaining (Fig.2-C). CD56 immunostaining also revealed numerous intramuscular nerve bundles and vertically infiltrating nerve fibers plus non-myelinated nerves in the muscularis mucosa, some of which infiltrated into the deep mucosal stroma (Fig. 2-D). Immunostaining for PGP 9.5 and NOS revealed more nerve fibers than by NF in the frozen sections (Fig. 2-E and -F). By contrast, routinely paraffin-embedded sections showed less scattered submucosal nerve fibers and myelinated intermuscular nerve bundled by PGP 9.5 and NOS immunostaining (Fig. 2-G and -H). Only a few nerve fibers were stained in the circular smooth muscle layer with paraffin-embedded sections (Fig. 2-G and -H). Spleen showed a few myelinated nerve fibers in the germinal center of the white pulp by NF staining (Fig. 3-A) while CD56 immunostaining revealed not only myelinated nerve fibers in the germinal center but diffusely, distributed non-myelinated nerve fibers in the arterial wall in the white pulp (Fig. 3-B). Pancreatic islets were faintly

immunostained by NF (Fig. 3-C) and stronger immunostained by CD56 (Fig. 3-D). Ganglion was noted close to the islets, which was surrounded by thin non-myelinated nerve fibers, some of which penetrated into the islets revealed by CD56 immunostaining but not by NF immunostaining (Fig. 3-C and -D). The cortex of kidney showed very few myelinated nerve fibers by CD56 staining and non-myelinated nerve fibers by NF immunostaining (Fig. 3-E and -F). The formalin-fixed and paraffin-embedded sections revealed large nerve bundles in the deep cortex with dense staining by PGP 9.5 but negatively stained by NOS, where scattered nerve fibers were noted plus mesangium being positively stained by PGP 9.5 (Fig. 3-G and -H). In thyroid, intrafollicular fibrous tissue contained many myelinated nerve fibers by NF staining, which were also immunostained by CD56 staining in addition to include the numerous non-myelinated nerve fibers infiltrating into the arterial media (Fig. 4-A and -B). In adrenal, myelinated nerve fibers were depicted in the subcapsular connective tissue and a few scattered non-myelinated nerve fibers were infiltrated continuo-usly through the cortex to the medulla by NF staining (Fig.4-C) while abundant non-myelinated nerves were located in the medulla, more by NF than CD56 staining (Fig. 4-C and -D). In urinary bladder, there were ample fragmented, mostly non-myelinated nerve fibers in suburothelial tissue and numerous, mostly myelinated nerve fibers in the smooth muscle layer accompanied with some small non-myelinated fibers by NF and CD56 immunostaining (Fig. 4-E and -F) where smooth muscle was moderately immunostained by CD56 (Fig. 4-F). Sections of vagina revealed nerve fibers adjacent to nerve plexus by NF immunostaining and numerous non-myelinated nerves in the submucosa by CD56 immunostaining (Fig. 4-G and -H). In the cycling endometri-um, Day 3 endometrium revealed non-myelinated nerve fibers by NF immunostaining and a few non-myelinated nerve fibers in the thin, sloughed off basalis compared to the much more numerous myelinated and non-myelinated nerve fibers in the myometrium (Fig. 5-A and -B). In Day 7 endometrium, a few non-myelinated nerve fibers were shown in the deep basalis by NF immunostaining (Fig. 5-C). In Day 28 endometrium, some small nerve fibers were also present in the deep and middle functionalis and numerous vertically arranged nerve fibers were present in the basalis (Fig. 5-D). The endometrium from the monkeys treated with ZK (an antagonist against progesterone) for 5 months revealed thickened basalis containing abundant non-myelinated nerve fibers by NF immunostaining and more numerous nerve fibers by CD56 immunostaining (Fig. 5-E and -F).

Discussion

Heart showed myelinated and non-myelinated nerve fibers in sub-epicardium by NF and intramuscular nerve fibers by CD56 immunostaining while there were a few penetrating small nerve fibers in the ventricle by CD56 staining around arterial adventitia (Fig. 1-A and -B). The cardiac autonomic nervous system plays to sustain the circulation of blood[28-31]. Beat-to-beat heartbeat was abolished by parasympathetic blockade but unblocked by sympathetic blockade [28]. Thus, cardiac autonomous system regulates all the crucial functions of the heart[28-31]. However, little is known about the distribution, morphology and immunohistochemistry of the nerve fibers in the human heart (32-34). Marron et al studied human heart with confocal and fluorescent microscopy and found nerve fibers (diameter, 6 to 10 µm) immunoreactive to myelin basic protein in the arterial endocardium and coronary sinus, which were immunoreactive to PGP 9.5, tyrosine hydroxylase and neuropeptide Y (NPY)[33]. Heart transplantation resulted in complete denervation of the donor heart with loss of afferent and efferent nerve connections including a complete absence of vagal nerve[33]. As a result, transplanted donor heart lost vagal tone and the heartbeat averages 90 beats/ min at rest[33]. Sympathetic reinnervation starts 6 months after transplantation[34] and evidence of reinnervation is usually found during the second year after transplantation and involves the myocardial muscle, sinoatrial node and coronary vessels but remains incomplete and limited many years post-transplantation[34-36]. In lung, a very few scattered non-myelinated nerve fibers were immunostained adjacent to the small arterial wall (Fig. 1-C and -D).
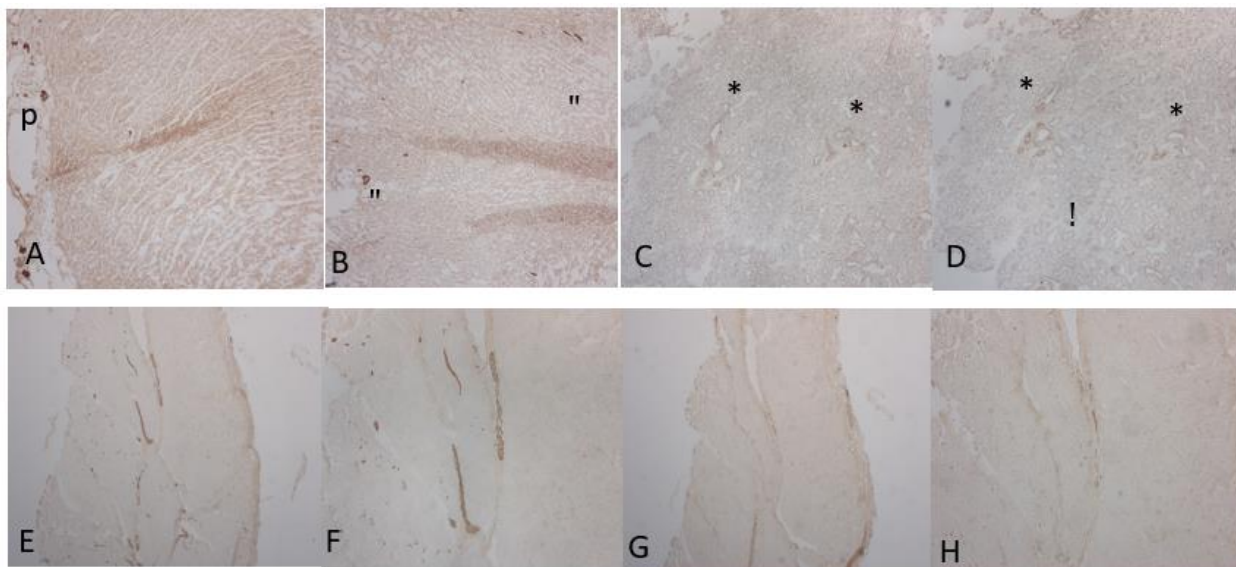
Figure 1. Heart, Lung and Diaphragm Several myelinated nerve fibers were depicted in the pericardium by NF immunostaining (**A**) while more small, myelinated and non-myelinated nerve fibers were present in the arterial adventitia in the ventricular wall by CD56 than NF immunostaining (**B**). In lung, a few periarterial non-myelinated nerve fibers were depicted by NF immunostaining (**C**) and more peri-arterial non-myelinated nerve fibers were revealed by CD56 immunostaining (**D**). In diaphragm, there were solid plexus of myelinated nerve fibers and scattered non-myelinated nerve fibers by NF immunostaining (**E and F**) and less plexus and non-myelinated nerve fibers were revealed by CD56 immunostaining in the fibrous stroma (**G and H**). p: pericardium, *: peri-bronchial nerve fiber, ": peri-arterial neve fiber

Using immunohistochemical staining, human lung showed PGP 9.5 immunostained in the cytoplasm of the subepithelial bodies and neuroendocrine cells of the respiratory epithelium[37]. Nerve fibers containing VIP-immunoreactivity were found in the human bronchial glands[38,39]. Fisher and Hoffman used NOS for immunostaining nerve fibers of the human airway including trachea, large and small bronchi and bronchioles and found NOS-positive nerve fibers decreased significantly from trachea to large-diameter bronchi to small-bronchi where NOS-nerve fibers were completely absent in the bronchi[40]. Our finding of very few NF and CD56 immunopositive nerve fibers corresponds to their findings. The cross sections of the diaphragm revealed contrasting findings between NF and CD56 immunostaining: NF immunostaining showed numerous plexuses, from which myelinated small nerve fibers were ramified by CD56 immunostaining (Fig. 1-E and -F). Plexuses probably represent motor neurons and small non-myelinated nerves may represent sensory nerves [41,42]. The phrenic nerve consists of motor, sensory and sympathetic nerve fibers and provides innervation to the diaphragm and

sensation to the central tendons part of the diaphragm[43]. Vagal sensory and motor neurons innervate crural diaphragm and pharyngo-esophageal ligament[44]. Crural diaphragm-vagal afferents show distortion of the gastro-esophageal junction, while vagal motor neurons innervate both crural diaphragm and distal esophagus [44]. The frozen sections of duodenum showed intermuscular plexus, from which submucosal plexus were derived and numerous non-myelinated nerve fibers penetrated through the circular inner smooth muscle as immunestained by NF and CD56 (Fig. 2-A and -B). There were many non-myelinated nerve fibers in the muscularis mucosa, from which a few smaller nerve fibers innervated into the lamina propria (Fig. 2-A and -B). We could not obtain good sections of large intestine, which also revealed the intermuscular Auerbach's plexuses and submucosal Meisner's plexuses by both NF and CD56 staining with more fine non-myelinated nerve fibers by CD56 than NF immunostaining (Fig. 2-C and -D). Paraffin-embedded sections of large intestine showed both Auerbach's and Meisner's plexuses with fewer longitudinally infiltrating small nerve fibers by PGP 9.5 immunostaining and less nerve fibers by NOS immunostaining (Fig. 2-G and -H). The superior immunostaining with frozen sections was demonstrated compared to the paraffin-embedded sections regarding much more immunostained small nerve fibers in the frozen sections with CD56 presenting as the best immunostaining, followed by PGP 9.5 and NOS and the least with NF immunostaining (Fig. 2-A to -F). PGP 9.5 is a cytoplasmic protein, which was initially isolated from brain-extract and is specific for neurites, neurons and cells of the diffuse neuroendocrine system at all stages differentiation[16,17]. PGP 9.5 has been used as a universal marker for all sensory nerve fibers of small-diameter fibers transmitting pain, and large-diameter fibers transmitting proprioception and motor fibers[16,17]. However, PGP 9.5 immunostaining with paraffin-embedded sections did not immunostain as many small nerve fibers as compared to NF and CD56 immunostaining in the frozen sections (Fig. 2-E to -H).The submucosal plexuses sense the lumen environment and regulate gastrointestinal blood flow and controlling the epithelial cell function and secretion. Three classes of enteric neurons are identified including motor neurons, intrinsic primary afferent neurons and interneurons. Intrinsic primary afferent neurons are primary sensors and regulate the enteric neuron system that detect the chemical features of the luminal content and physical states of the small intestine[45-49]. In large intestine, Auerbach's myenteric plexuses provide motor innervation to both smooth and secretomotor innervation to the mucosa with both parasympathetic and sympathetic functions[50]. Meissner's sub-mucosal plexus has only parasympathetic fibers, which are located in the submucosa and its nerve fibers are finer than myenteric plexuses of Auerbach's and innervates into lamina propria as seen in the photomicrographs (Fig. 2-A and -B).

The main function of the large intestine is to absorb water and any remining absorbable nutrients before sending the indigestible matter to the rectum. The large intestine absorbs vitamins such as thiamine, riboflavin and vitamin K that are created by colonic bacteria[50]. Thus, intestines are richly innervated for peristalsis, absorption of nutrients and water and enteric hormone homeostasis. Spleen is diffusely innervated by small, fragmented, non-myelinated nerve fibers as revealed by CD56 immunostaining while NF immunostaining showed only small fragmented myelinated nerve fibers in the germinal center (Fig. 3-A and -B). Sympathetic nerve fibers were immunostained by tyrosine hydroxylase and were richly innervated in the while pulp, distributing into marginal sinus and parafollicular zone[51]. Using immunofluorescent staining for NF, nerve fibers were found in all compartments including the splenic nodules, lymphoid sheath, marginal zone, trabeculae and pulp[51-53]. Thus, spleen is richly and diffusely innervated by small nerve fibers and the nerve fibers may contribute to the production of antibodies to the circulating antigens [52,53]. Pancreas was diffusely innervated by small, non-myelinated nerve fibers in the exocrine pancreas and these small, non-myelinated nerve fibers surrounded the islets, some of which penetrated into the islets revealed only by CD56 immunostaining (Fig. 3-D)[54-57].
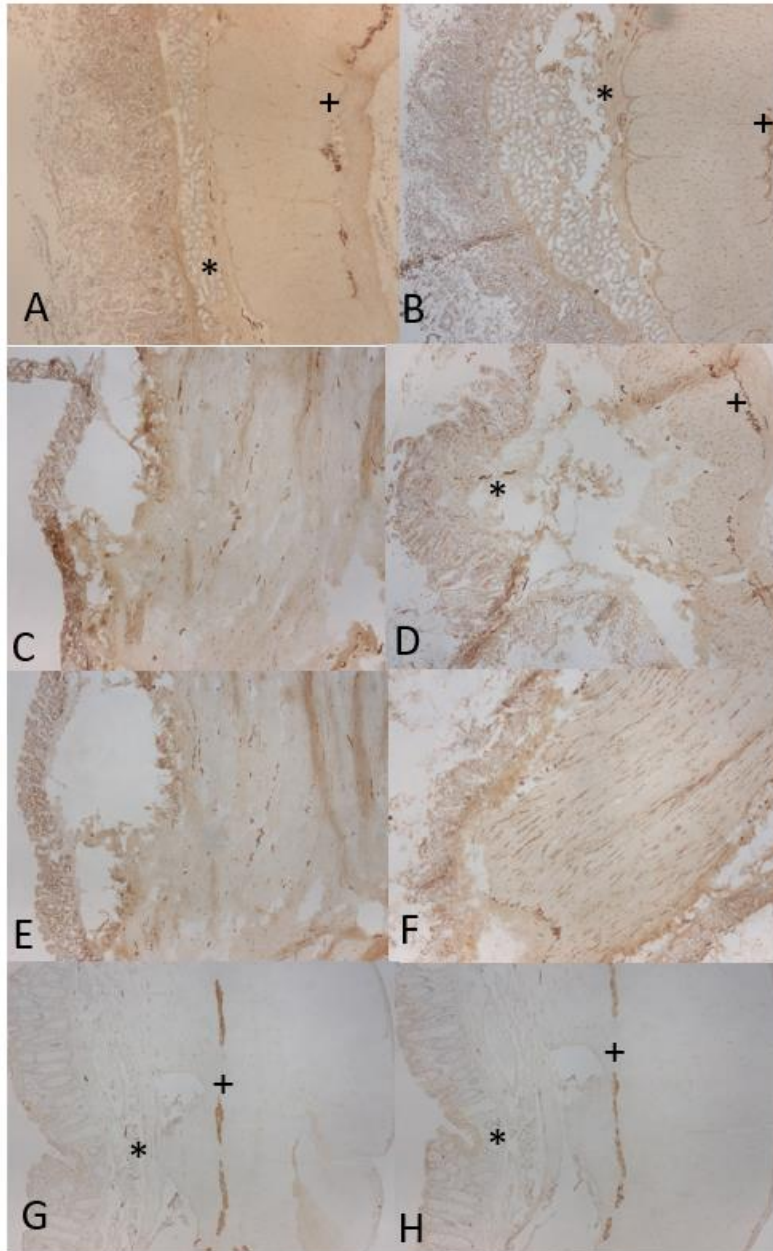
Figure 2. Duodenum and Large Intestine In duodenum, there were scattered myelinated submucosal plexus (Meissner's) and solid, myenteric nerve plexus (Auerbach's) between the inner and outer smooth muscle layers equally by NF and CD56 immunostaining (**A and B**). In large intestine, in addition to Meissner's and Auerbach's plexuses, scattered myelinated submucosal and intermuscular layer nerve fibers were depicted by NF immunostaining (**C**) as compared to more nerve fibers by CD56 immunostaining, some of which penetrated into the deeper lamina propria (**D**). There were much less nerve fibers by PGP 9.5 immunostaining (**F**) than by NOS immunostaining(**H**) in large intestine. In paraffin-embedded sections of large intestine, there were some submucosal plexus and abundant myenteric plexuses while there were less myelinated nerve fibers in the smooth muscular layer and there were a few non-myelinated nerve fibers in the inner circular and outer longitudinal muscular layers by both PGP 9.5 (**G**) and NOS (**H**) immunostaining by the paraffin-embedded sections. ∗: Meissner's plexus, +: Auerbach's plexus

Ganglion was located in the proximity to the islets and was immunostained for both NF and CD56 with darker staining with CD56 than with NF (Fig. 3-C and -D). Insulin secretion has two phases in response to glucose infusion in vivo: the early cephalic phase takes place within 5 min and the second phase occurs after 20 min after glucose infusion[58]. In cephalic phase in vivo, the mere presence of food in the mouth, which does not increase blood glucose, results in an increase of insulin secretion[59,60]. In this phase, vagal motor neurons mainly stimulate insulin secretion while sympathetic motor neurons mainly stimulate glucagon secretion[59]. In the perfused pancreas and perifused isolated islets in

vitro, the first phase of glucose-induced insulin secretion is mediated through glucose receptor and glucose transporter system, through which glucose modulates insulin secretion[58,61]. Pancreatic polypeptide secretion is also mediated through autonomous nerve system in the cephalic phase of secretion[60]. Thus, both intrapancreatic nerve fibers and ganglia have an important influence on pancreatic hormones secretions[59-62]. Frozen sections of kidney cortex showed a few myelinated nerve fibers around the small arteries by CD56 immunostaining and non-myelinated fibers by NF immunostaining (Fig.3-E

and -F). Kidney tissue was also fixed in a mixture of paraformaldehyde and formaldehyde and were embedded in paraffin, and these sections were immunostained for PGP 9.5 and NOS: many myelinated and non-myelinated nerve fibers were noted in the medium-sized arterial wall (Fig. 3-G and -H). A few spotty positive staining was observed in the hilus of the glomerulus, corresponding to the JG apparatus, and small PGP 9.5 -positive nerve fibers adjacent to the small arterial wall and the collecting tubule in the deep cortex, which were not revealed by NF immunostaining (Fig. 3-G and -H).
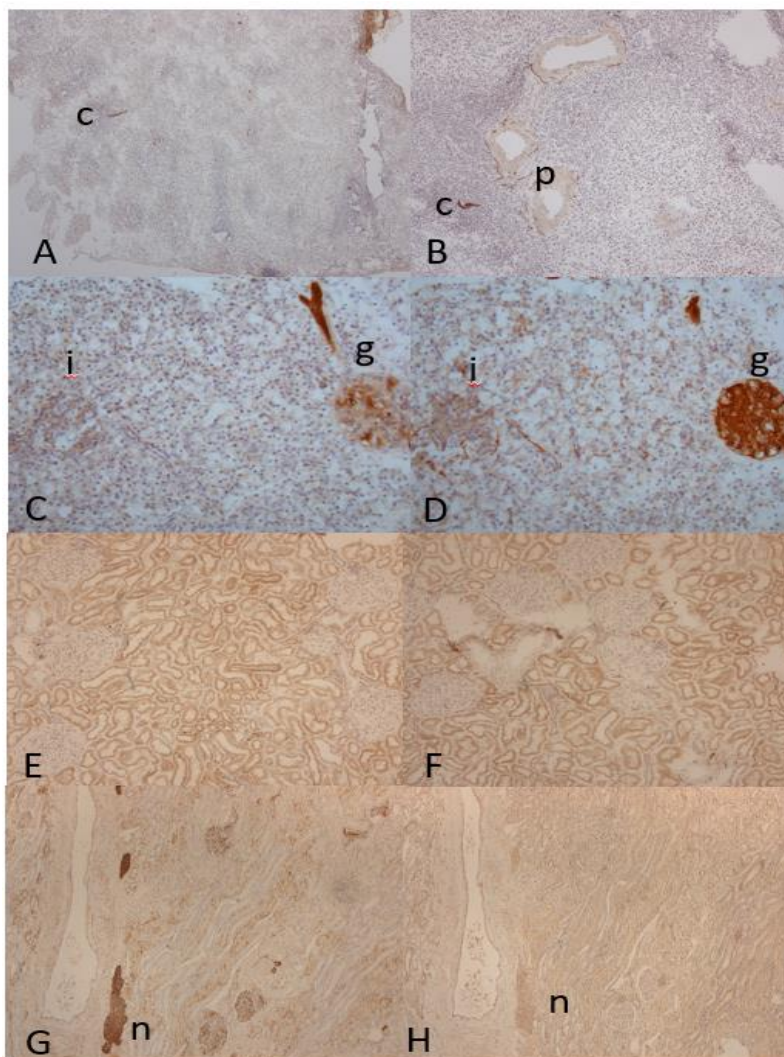

Figure 3. Spleen, Pancreas and Kidney In spleen, there were a few myelinated nerve fibers in the germinal center by NF and CD56 immunostaining with additional abundant, small non-myelinated fibers in the arterial wall by CD56 immunostaining (**A and B**). In pancreas, ganglion was weakly immunostained by NF (**C**) and strongly immunostained by CD56 (**D**). CD56 immunostained diffusely scattered non-myelinated nerve fibers in the inter-acinar stroma, some of which circled and penetrated into the islets (**D**), which were not immunostained by NF immunostaining (**C**). In kidney, there were a very few myelinated nerve fibers in the peri-glomerular arterial adventitia by both NF and CD56 immunostaining (**E and F**). In the paraffin-embedded sections of kidney, large, myelinated nerve bundles were depicted adjacent to the artery by PGP 9.5 immunostaining (**G**), which were not immunostained by NOS (**H**). c: geminal center, g: ganglion, i: islet of Langerhans, n: nerve bundle

Sympathetic nerve fibers innervate both vascular and tubular structures throughout the kidney tissue except in the inner medulla[63-66]. All parts of the renal vasculatures are innervated with the greatest density along the afferent arterioles[63,65,66] as observed by PGP 9.5 staining in the paraffin-embedded sections[63-65]. Innervation of major renal components including blood vessels, tubules, pelvis and glomerular forms a bidirectional neural network to relay blood flow, glomerular filtration rate, tubular resorption of sodium and water and release of renin and prostaglandins, which contribute to cardiovascular and renal regulation[66]. Thus, autonomous nerve has some control on the kidney function[64,65]. Renal nerve activity is commonly increased in pathophysiological conditions such as hypertension and chronic and end-stage renal diseases[65,66]. Interfollicular septum of the thyroid gland contained myelinated nerve fibers by both NF and CD56 immunostaining (Fig. 4-A and -B). Small non-myelinated nerve fibers penetrated into the tunica media of artery, which was more clearly shown by CD56 immunostaining than NF immunostaining (Fig. 4-A and -B). PGP 9.5-positive nerve fibers were detected in the various thyroid lesions including the normal thyroid, papillary and follicular carcinoma and majority were adrenergic although minor cholinergic innervation was detected in the interfollicular stroma[67]. Thyroid sympathetic adrenergic nerve terminals were found at the network around the blood vessels and also as single terminals between follicles as revealed using acetylcholine esterase histochemistry[68] and immunohistochemical staining for neuropeptide Y[69]. Sympathetic nerve activation appears to induce thyroid hormone secretion by a direct activation of norepinephrine from the intrathyroidal sympathetic fibers[70]. The cortex and medulla of adrenal gland has been traditionally regarded as independent entities[71]. Adrenal gland had myelinated nerve fibers in the sub-capsule, from which a few non-myelinated nerve fibers penetrated into the cortex, continuously to the medulla by more staining by NF than CD56 immunostaining (Fig. 4-C and -D). There were numerous thin non-myelinated nerve frameworks in the medulla filling the entire space (Fig. 4-C and -D). The literature has shown that nerve fibers are sparse in the adrenal cortex and are confined to the vicinity of blood vessels[72]. Many nerve fibers of adrenal gland enter the gland through its hilus, and medial margin and the majority of nerve fibers enter the gland in the medulla, where they ramify and give off fibers that mostly terminate with chromaffin cells. Nerve fascicles derived from subcapsular plexuses penetrate cortex to run alongside arterioles in the cortex to the medulla[73]. In the subcapsular region, myelinated and non-myelinated nerve fibers were found, and terminal axons were present in zona glomerulosa, and nerve bundles were most commonly found in zona fasciculate, and axon terminals were in the close proximity to chromaffin cells[74]. Using immunohistochemical staining for substance P and NOS, Heym et al and others found substance P and NOS staining in the adrenal cortex while all other nerve fibers were noted in both cortex and medulla[75,76]. Adrenal medulla received sympathetic and parasympathetic efferent and afferent innervations[75,76]. Adrenal medulla is modified post-ganglion neuron and preganglionic autonomic nerve fiber and secretes catecholamines including epinephrine, norepinephrine and small amount of dopamine in response to stimulation by sympathetic preganglionic neurons[76]. Urinary bladder showed a striking difference of innervations between the suburothelial tissue and smooth muscle layer. There were mostly non-myelinated nerve fibers in suburothelial tissue by NF and CD56 immunostaining while there were mostly myelinated nerve fibers in smooth muscle layer by NF and CD56 immunostaining (Fig. 4-G and -H). Smooth muscle of urinary bladder was moderately immunostained by CD56, while smooth muscles of intestines were negatively stained by CD56 (Fig. 4-F). CD56 is also known to stain young, striated muscle cells[20]. Control of bladder and urethral outlet is dependent on three sets of peripheral nerves: parasympathetic, sympathetic and somatic nerves that contain afferent and efferent pathway[79]. Afferent nerves innervating the bladder have Adelta and C-fiber axons while storage and voiding reflexes are activated by mechanosensitive Adelta afferent nerves that respond to bladder distention[79,80]. C-fibers are non-myelinated axons, which innervate mostly in the suburothelial tissue and Adelta fibers are myelinated axons, which innervate mostly in the smooth muscle layer[78]. Parasympathetic preganglionic nerve terminals release acetylcholine, which can excite various muscarine receptors in bladder smooth muscle, leading to bladder contraction[77-80]. Pelvic nerve afferents, which monitor the volume of bladder and the amplitude of bladder contraction, consist of small myelinated Adelta-fibers and unmyelinated C-fibers. Normal micturition reflex is mediated by myelinated Adelta-fibers in the smooth muscle layer, that respond to distention[79]. Our study immunostained mostly non-myelinated nerve fibers in the suburothelial tissue and myelinated nerve fibers in the mostly smooth muscle layer corresponding to the functional study of the nerve fibers in the suburothelial tissues and smooth muscle layer, respectively[78]. Sections of vagina revealed numerous non-myelinated and myelinated nerve fibers in the submucosa by CD56 immunostaining while nerve plexuses and many myelinated nerves were depicted in the deep

connective tissue by NF immunostaining (Fig. 4-G and -H).
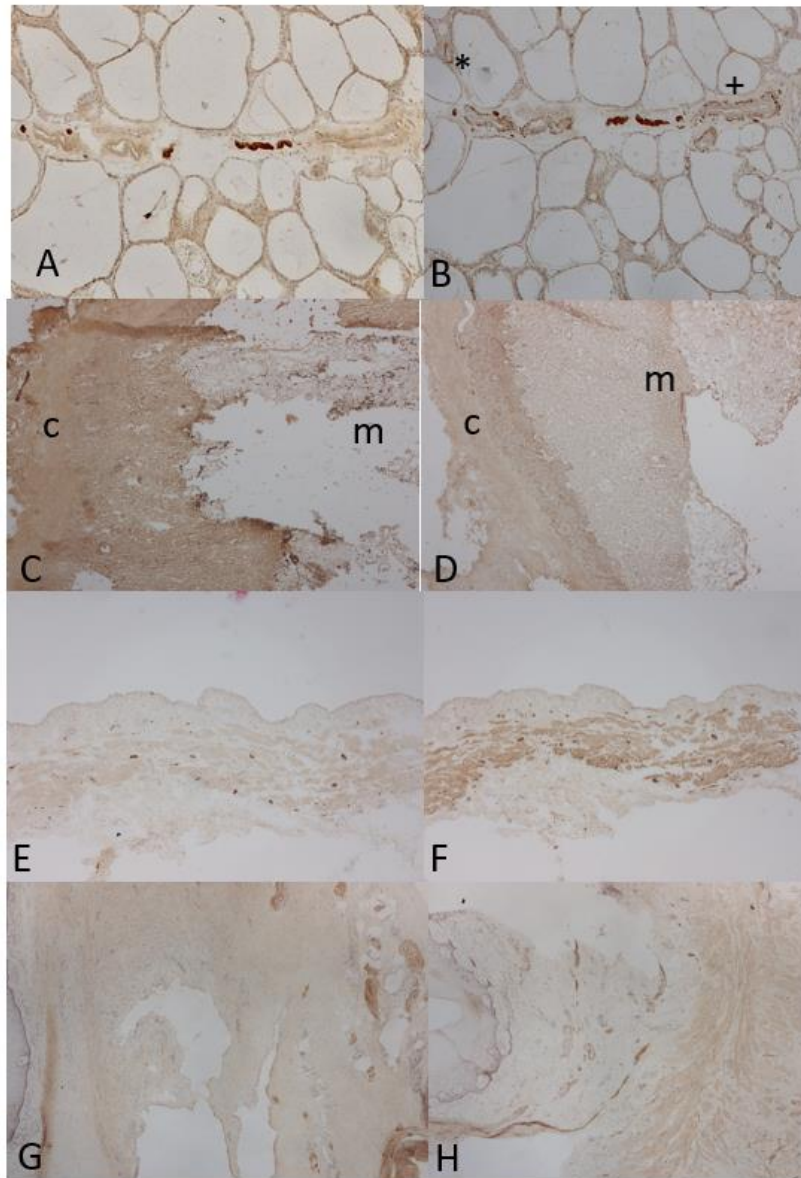
Figure 4. Thyroid, Adrenal Gland, Urinary Bladder and Vagina In thyroid, myelinated nerve fibers were depicted in the interfollicular stroma by NF and CD56 immunostaining (**A and B**) and there were penetrating, abundant non-myelinated nerve fibers in the arterial wall by CD56 immunostaining (**B**). In adrenal gland capsule, there were myelinated nerve fiber, and in the cortex, there were a few non-myelinated nerve fibers and numerous non-myelinated nerve fibers in the medulla by NF immunostaining (**C**). CD56 immunostaining showed a few myelinated nerve fibers in the capsule and in the deep cortex, and many non-myelinated nerve fibers in the medulla (**D**). In urinary bladder, scattered mostly non-myelinated nerve fibers in the suburothelial tissue and abundant, mostly myelinated nerve fibers in the smooth muscle layer by both NF and CD56 immunostaining (**E** and **F**). Smooth muscle in the urinary bladder was moderately stained only by CD56 (**F**). Vagina showed numerous myelinated nerve plexus in the deep connective tissue by NF immunostaining (**G**) while several non-myelinated nerve bundles and scattered non-myelinated periarterial non-myelinated nerve fibers were present in the superficial submucosa by CD56 immunostaining (**H**). c: capsule, m: medulla, ∗: interfollicular nerve fibers, +: periarterial nerve fiber

Functional studies provided evidence that sympathetic nerves were excitatory to vagal non-vascular smooth muscle while NOS-positive nerves appeared to mediate muscle relaxation and vasodilation[81]. With formalin-fixed and paraffin-embedded sections of human vagina, Hoyle et al and others found the relative density of nerve markers as follows: PGP 9.5 > vasoactive intestinal polypeptide (VIP) > NOS[81]. Li et al studied nerve fibers from the biopsied different locations of human vagina using

immunohistochemical staining for PGP 9.5 with formalin-fixed and paraffin-embedded tissues[82]. They found a considerable difference in nerve distribution in the human vagina: vaginal innervation was observed in the lamina propria and muscle layer of the anterior vaginal wall. The distal wall of the anterior vaginal wall had significantly richer small verve fibers in the lamina propria than the proximal third and in the virginal muscle layer [83]. More recently, Griebling et al fixed vaginal biopsy specimen in Zamboni' solution at 4°C and washed for 7 days with PBS at pH 7.4 and stored at -80°C until frozen sectioned at 10 μm. Women not receiving hormone therapy showed relatively high levels of innervation by tyrosine hydroxylase and VIP immunostaining than women receiving hormone therapy[84]. The presence of nerve fibers in the endometrium has been debated. In most mammalian species, the endometrium is poorly innervated by autonomic and efferent nerve fibers, and these nerves are associated with blood vessels[85]. Sympathetic nerves approach endometrial glands, suggesting a role in endometrial secretion. Parasympathetic nerves rarely penetrate deeply in the endometrium and do not associate with endometrial glands[83]. Our results of nerve fibers in the secretory phase endometrium may support growing nerve fibers in the functionalis of secretory phase from basalis, which may have a role in endometrial secretion and pain during menstrual cycle. In rhesus monkey endometrium, fragmented non-myelinated nerve fibers were present in the basalis of in Day 3 cycling endometrium by NF immunostaining (Fig. 5-A). In Day 7 proliferative phase, there were some longitudinal, small nerve fibers in the basalis but not in the thin functionalis, and there were a few small nerve fibers at the deep functionalis, suggesting that nerve fibers grew from the basalis into functionalis in Day 7 to Day 21 (Fig. 5-B and -C). In Day 28 endometrium during the menstrual cycle, new nerve fibers penetrated into mid-portion of enlarging functionalis (Fig. 5-C and -D). The ZK treated monkeys for 5 months, which showed extremely thickened basalis, revealed more, small nerve fibers by CD56 immunostaining than by NF immunostaining (5-E and -F). In the cycling human endometrium, from proliferative to secretory phase, the growing nerve fibers were observed from basalis to lower functionalis and then, into deeper functionalis to upper functionalis using alkaline phosphatase as the final visualization for NF and CD56[13]. Tokushige et al used formalin-fixed and paraffin-embedded human endometrial sections using PGP 9.5, NF, VIP, substance P,

tyrosine hydroxylase and others, and studied the distribution of nerve fibers in the human endometrium from women with endometriosis[4].They found more nerve fibers in the functionalis from women with endometriosis, which decreased by hormonal treatment[4,5,7]. There was no mention on menstrual cycle of tissue studied for endometriosis. If our results were right, nerve fibers grow in the secretory phase of menstrual cycle. A similar study was also reported by Boker et al with routinely paraffin-embedded sections using PGP 9.5, VIP and substance P[5]. These authors published limited, small tissue areas of positively stained photomicrographs without presenting low power photomicrographs, possibly selecting positively stained microscopic areas. With routinely paraffin-embedded tissues, reliable immunohistochemical staining for nerve fibers is technically difficult since nerve fiber antigens are expressed at low levels in the majority of normal organs except brain and spinal cord[2,3]. With human hysterectomy specimen, which had been fixed in Bouin's fixative and paraffin-embedded sections, Sparzio Sardo et al performed immunohistochemical staining using S-100, neuron specific enolase (NSE) and others as nerve markers: nerve fibers were depicted at the level of functionalis and adnomyosis[86]. Adequate immunostaining for nerve fibers was only feasible with frozen tissues, which were frozen sectioned and were stained for nerve fiber markers as described in the nerve fibers in the skin as described below. Skin punch biopsy with the assessment of intradermal sensory nerve fibers using pan-axonal marker, PGP 9.5 is an established clinical and research technique, and this technique may also be used to assess other population of nerve fibers in other tissues[87,88]. Another method uses initially fixed tissues, which are later frozen sectioned and the floating 50 μm sections were immunostained for nerve fibers markers to increase the visibility of the scarcely innervated nerve fibers since thicker tissue sections increase the chance to observe denser nerve fibers (89). The endometrium, especially those of the secretory phase, is so edematous and fragile that the fixed floating 50 μm sections are extremely difficult to process for immunohistochemical staining for frozen sectioning at our hand. The advantages of using frozen sections for immunohistochemical staining were depicted especially in the sections of intestines, diaphragm and pancreas. In intestines, fine motor nerve fibers were clearly and abundantly demonstrated at such a level compared to less nerve fibers immunostained in the paraffin-embedded sections (Fig. 2-A to -H).
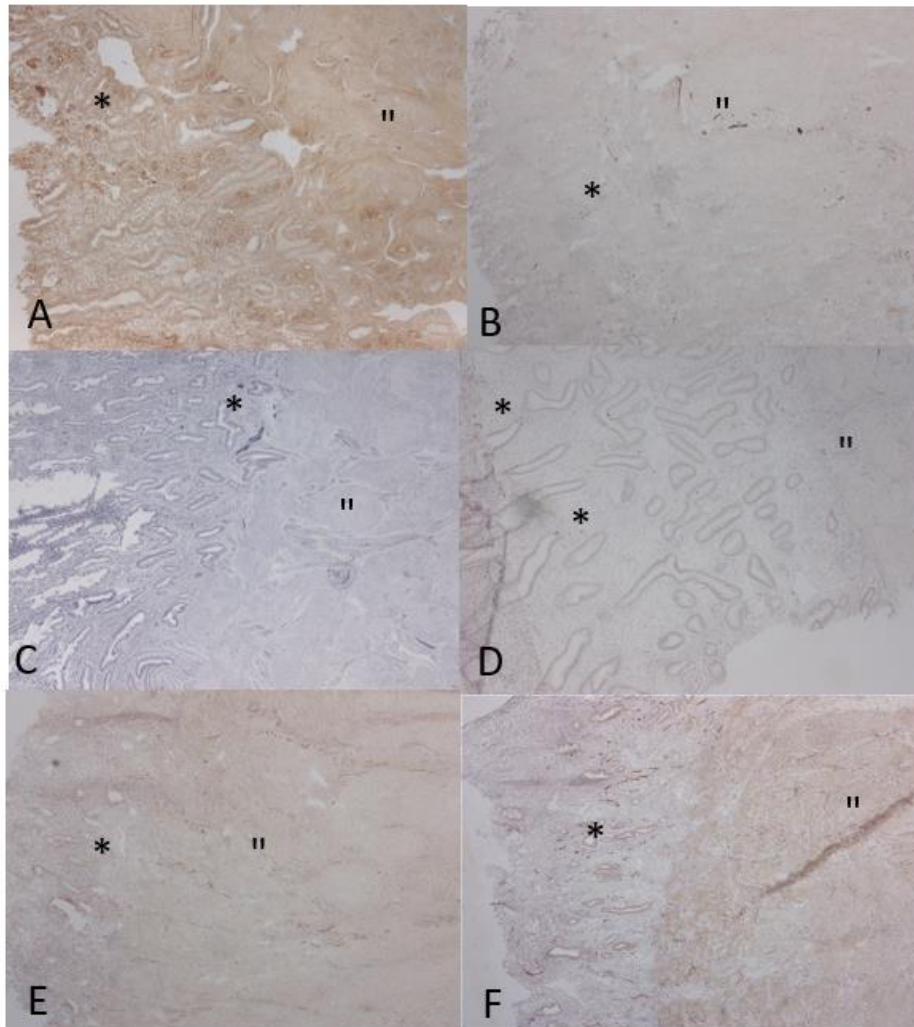
Figure 5. Endometrium Day 3 endometrium showed thin sloughed off basalis where there were non-myelinated nerve fibers in the deep basalis and myometrium (**A**). In Day 7 endometrium, there were few non-myelinated nerve fibers at the deep basalis and a very few nerve fibers in the middle-basalis (**B**). In Day 21 enlarging endometrium, there were more increased nerve fibers in the deep basalis plus a few nerve fibers in the mid-basalis (**C**), which was immunostained using alkaline phosphatase method. In Day 28 more enlarging endometrium, there were more nerve fibers in mid basalis and a few in the enlarged deep functionalis (**D**). Day 3 to Day 28 endometrium was immunostained by NF. Endometrium from monkeys treated with ZK for 5 months revealed much thickened basalis containing numerous non-myelinated nerve fibers in the entire basalis as much as in the myometrium by NF immunostaining (**E**) while there were much more non-myelinated nerve fibers revealed in the entire thickness of the basalis by CD56 immunostaining than NF immunostaining (**F**). ∗: nerve fibers in mucosa, ": nerve fibers in myometrium

In pancreas, ample, delicate fine nerve fibers were extensively depicted in the frozen sections, some of which surrounded the islets and penetrated into the islets in a proximity of ganglion by CD56 but not by NF immunostaining (Fig. 3-C and -D), which had not been depicted in the paraffin-embedded sections. NF has been widely used for immunohistochemical staining for nerve cells and nerve fibers, but CD56 has not been extensively used for nerve fibers. CD56 is an excellent marker for nerve fibers, sensory nerve binding and ganglion cells[20]. Iwami et al immunostained nerve fibers around the branches of hepatic arteries, portal veins and bile ducts in the portal area using CD56[90]. Using tyrosine hydroxylase, NPY and VIP as nerve fiber markers, Ariyoshi et al also detected nerve fibers in the proximity of hepatic arteries, portal veins and bile ducts with formalin-fixed and paraffin-embedded sections of human liver[91]. More recently, Grant et al observed nerve fibers in the macaque liver in close contact with portal triads, central veins and parallel with liver sinuses[92]. Thus, nerve fibers are diffusely distributed in the liver as similarly diffusely observed in the spleen and pancreas (Fig. 3-A to -D). The hindside of frozen section immunostaining is that this procedure is labor-intensive and cumbersome and further, only small tissues (1 x 1 x 0.4 cm) are adequately processed in our hand[12-14]. During

the freezing process, the tissue may break or crack, the larger tissues tend to crack more often than the smaller tissues. The frozen tissue sections mounted on the glass slide may degenerate when they are stored for some time even stored at -70°C, so, the frozen sections should be used for immunostaining as soon as possible. For a practical purpose in detecting nerve fibers at a diagnostic pathology laboratory, PGP 9.5 immunostaining with formalin-fixed and paraffin-embedded sections would be adequate for routine diagnosis for general anatomic pathologists [93,94].

Conclusion

Frozen section immunohistochemical staining has validated this technique's superiority over the formalin-fixed and paraffin-embedded tissue sections for immunostaining nerve fibers as also this technique's superiority has been previously proved for immunostaining lymphatic and blood vessels (11-13). The new findings using frozen sections immunostaining will eventually shed light more on the basic histology and histopathology in normal and pathological tissues.

References

1. Kerr, JB: Nervous system. In : Kerr, JB, Atlas of Functional Histology, ed. JB Kerr, Mosby, London, 1998; 107-110.

2. Litchfield, S, Nagy, Z: New treatment modification makes the Bielschowsky silver stain reproducible. *Acta Neuropath* 2001(1);17-21.

3. Uchihara, T: Silver diagnosis in neuropathies: principles, practice and revised interpretation. *Acta Neuropath* 2007, 113(5);483-499.

4. Tokushige, N, Marham, R, Russell, P, Fraser, IS: High density of small nerve fibers in the functional layer of the endometrium in women with endometriosis. *Hum Reprod* 2006, 21(3);782-787.

5. Tokushige, N, Markham, R, Russell, P, Fraser, IS: Different types of small nerve fibers in eutopic endometrium and myometrium in women with endometriosis. *Fert Steril* 2007, 88(4);795-803.

6. Boker, A, Kyama, CM, Vercruysse, L, Fassbender, Gevaert, O et al: Density of small diameter sensory nerve fibers in endometrium: a semi-invasive diagnostic test for minimal to mild endometriosis. *Human Reprod* 2009, 24(12);3025-3032.

7. Tokushige, N, Markham, R, Russell, P, Fraser, IS: Effects of hormonal treatment in nerve fibers in endometrium and myometrium in women with endometriosis. *Fertil Steril* 90(5);1589-1598.

8. McArthur, JC, Stocks, EA, Hauer, P, Cornblath, DR, Griffin, JW: Epidermal nerve fibers density. *Arch Neurol* 1998, 55(12);1513-1520.

9. Ebenzer, GS, Hauer, P, Gibbons, C, McArthur, JC, Polydefkis, M: Assessment of epidermal fibers: A new diagnostic and predictive for peripheral neuropathies. J Neuropath *Exp Nerol* 2007, 66(12);1059-1073.

10. Saperstein, DS, Leveine, TD, Hank, N: Usefulness of skin biopsy in the evaluation and management of patients with suspected small nerve neuropathy fiber neuropathy. *Int J Neurosci* 2013,123(1);38-41.

11. Grayston, R, Czanner, E, Elhadd, K, Goebel, A, Frank, B et al: A systematic review and meta-analysis of the prevalence of small fiber in pathology in fibromyalgia of a new paradigm in pathology in fibromyalgia etiogenesis. *Sem Arthritis Rheumat* 2019, 48(5);933-949.

12. Tomita, T, Mah, K: Cyclic changes of lymphatic and venous vessels in human endometrium. *Open J Pathol* 2014, 4(1);5-12.

13. Tomita, T, Mah, K: Cyclic changes of nerve fibers in human endometrium. *Open J Pathol* 2014, 4(1);68-78.

14. Tomita, T: Immunohistochemical staining for lymphatic and blood vessels in normal tissues: comparison between routinely paraffin-embedded tissues and frozen sections. *Acta Medica Acad* 2120, 50(1);13-28.

15. Thompson, RS, Doran, JF, Jackson, P, Dhillon, AP, Rode, J: PGP9.5 -A new marker for vertebrate neurons and neuroendocrine cells. *Brain Res* 1983, 278(1-2);224-228.

16. Wilkinson, KD, Lee, KM, Deschpande, S, Deschpande-Hughs, P, Boss, JM: The neuron specific protein PGP9.5 is ubiquitin carboxy-terminal hydroxylase . *Science* 1989, 246(4930);670-673.

17. Karanth, SS, Springall, DR, Kuhn, DM, Levine, MM, Pollak, JM: An immunocytochemical study of neuropeptides and protein gene 9.5 in man and common employed laboratory animals. Am J Anat, 1991, 191(4);369-383.

18. Schlepfer, WW: Neurofilaments: structure, metabolism and implications in disease. *J Neuropathol Exp Neurol* 1987, 46(2):117-129.

19. Yuan, A, Rao, MV, Veeranna, Nixon, RA: Neurofilaments at a glance. *J Cell Sci* 2012, 125(14);3257-3263.

20. Hall, J: Guyton and Hall Textbook of Medical Physiology, 12th ed., Saunders/Elsevier, Philadelphia, PA, 2011, 563-564.

21. Nagi, SS, Marshall, AG, Makdani, MA, Jarocha, E, Lifjencranz, J et al: An ultrafast system for signaling mechanical pain in human skin. *Sci Adv* 2019, 5(7);1297.

22. Mechtersheimer, G, Stauder, M, Moller, P : Expression of the natural killer cell--associated antigen CD56 and CD57 in human neural and striated muscle cells and their tumors. *Cancer Res* 1991, 51(5);1300-1307.

23. Jensen,M, Berthold, F: Targeting the neural cell adhesion in molecules in cancer. *Cancer Lett* 2007, 258(1);9-21.

24. Enriquez-Barreto, L, Palazzetti, C, Brenonann, LH, Maness, PF, Fairen, A: Neural cell adhesion in molecule, NCAM, regulates thalamocortical axon pathfinding and the organization of cortical somatosensory regeneration in mouse. Fron Molec Neurosci 2012, 00076.

25. Leshcynska, I, Liew, HT, Shephard, C, Halliday, GM, Stevens, CH: Aβ-derived reduction of MCA M2 -mediated synaptic adhesion contributes to synaptic loss in Alzheimer's disease. *Nature Common* 2015, 6;8836.

26. Lajoix, AD, Reggio, H, Chardes, T, Peraldi-Roux, S, Tribillac, E et al: A neural isoform of nitric oxide synthase expression in pancreatic β-cells control insulin secretion. *Diabetes* 2001, 5(6);1311-1323.

27. Bahadoran, Z, Caristyrom, M, Mirmiran, P, Ghasemi, A: Nitric oxide: To be not to be

endocrine hormone? *Acta Physiolo* 2020,229(1);e13443.

28. Wheeler, T, Watkins, PS: Cardiac denervation in diabetes. *Br J Med* 1973, 4;584-586.

29. Marron, K, Wharton, J, Shepard, MN, Fagan, D, Royston, D et al: Distribution, morphology, and neurochemistry of endocardial and epicardial nerve terminal arborization in the human heart. *Circulation* 1995, 92(8);2343-2351.

30. Armour, JA, Murphy, DA, Yuan, BX, MacDonald, S, Hopkins, DA: Gross and microscopic anatomy of the human intrinsic cardiac nervous system. *Anat Rec* 1999, 247(2);289-298.

31. Michell, GA: Innervation of the heart. *Br Heart J*, 1953,15(2);159-171.

32. Cavallotti, C, Bruzzone, P, Mancone, M: Catecholaminergic nerve fibers and beta-adrenergic receptors in the human heart and coronary vessels. *Heart Valves* 2002, 17(1);30-35.

33. Hanna, P, Rajendran, PS, Ajiola, O, Vaseghi, M, Andrew, J et al: Cardiac neuroanatomy-imaging nerves to define functional control. *Auton Neurosci* 2017,207;48-58.

34. Christensen, AH, Nygaard, S, Rolid, K, Nytroen, K, Gullestad, L et al: Early signs of sinoatrial reinnervation in the transplanted heart. *Transplantation* 2021, 105(9);2086-2096.

35. Grupper, E, Gewirtz, H, Kushwaha, S: Reinnervation post-transplantation. *Eur J Heart*, 2018, 39(20);1799-1806.

36. Crick, SJ, Wharlton, J, Sheppard, MN, Royton, D, Yacoub, MH et al: Innervation of the human cardiac conduction system: A quantitative immunohistochemical and histochemical study. *Circulation* 1994, 89(4);1697-1708.

37. Sparrow, MP, Weichselbaum, M, McCry, B Jr: Development of the innervation and airway smooth muscle in human fetal lung. *Am J Respir Cell Mol Biol* 1999, 20(4);550-560.

38. Lauwryns, JM, Van Ranst, L: Protein gene product 9.5 expression in the lungs of humans and other mammals. Immunocytochemical detection in neuroepithelial bodies, neuroendocrine cells and nerves. *Neurosci* 1988, 85(3);311-316.

39. Laitinen, A: Autonomic innervation of the human respiratory tract as revealed by histochemical and ultrastructural method. *Eur J Respir Dis* 1985, 140(Suppl);1-42.

40. Fisher, A, Hoffmann, B: Nitric oxide synthase in neurons and nerve fibers of lower airways and in vagal sensory ganglia of man. Correlations with neuropeptides. *Am J Respir Crit Med* 1996, 154(1);209-216.

41. Hiayet, MA, Wiid, HA, Wilson, AS: Investigations on the innervation of the human diaphragm. *Anat Rec* 1974, 179(4);507-516.

42. Martin, M, Li, K, Wright, MC, Lepore, AC: Functional and morphological assessment of diaphragm innervation by phrenic motor neurons. *J Vis Exp* 2015, 99;e52605.

43. Verlinden, TJM, van Djik, P, Herrier, A, de Gierde Vries, C, Lamers WH et al: The human phrenic nerve serves as morphological conduit for autonomic nerves and innervates the caval body of the diaphragm. *Scientific Rep*, 2018, 8;11697.

44. Young, RL, Page, AJ, Cooper, NL, Fishby, CL, Blickshow, LA: Sensory and motor innervation of the crural diaphragm by the vagal nerve. *Gastroenterol* 2010, 138(3);1091-1101.

45. Gazami, BA, Srinivassan, S: Enteric nerve system in the small intestine: Pathophysiology and clinical implication. *Curr Gastroenter Rep* 2010, 12(5);358-365.

46. Garcia-Victoria, M, Garcia-Corchon, C, Rodrigues, JA, Garcian-Amigot, E, Burrel, MA: Expression of neuronal nitric oxide synthase in several type of the rat gastric epithelium. *J Histochem Cytochem* 2000, 48(8);1111-1119.

47. Timermans, JP, Babiers, M, Scheurmann, DW, Bogers, JJ, Adriansen, D et al: Nitric oxide synthase immunoreactivity in the enteric nervous system of the developing human digestive tract. *Cell Tissue Res* 1994, 275(2);235-245.

48. Wattchow, DA, Brooks, SJ, Cost, M: The morphology and projections of retrogradely labelled myenteric neurons in the human intestines. *Gastroenterol* 1995, 109(3);866-875.

49. Porter, AJ, Wittchow, DA, Brooks, SIH, Schurmann, M, Costa, M: Choline acetyltransferase immunoreactivity in the human small and large intestine. *Gastroenterol* 1996, 111(2)401-408.

50. Assouz, LL, Sharma, S: Physiology, Large intestine. Stat Pearls, August 9, 2021.

51. Felten, DL, Ackerman, KD, Wiegand, SJ, Felten, SY: Noradrenergic sympathetic innervation of the spleen. 1. Nerve fibers associate with lymphocytes and macrophages in specific compartments of the splenic white pulp. *J Neurosci Res* 1987,181(1);28-36.

52. Bujis, R, van der Villet, J, Garidodus, ML, Huntinga, I, Escobar, C: Spleen vagal denervation inhibits the production of antibodies to circulating antigens. PLOS 3(9);e3152,2008.

53. Hu, D, Al-Shalan, MHA, Shi, Z, Wang, P, Wu, Y et al: Distribution of nerve fibers and nerve-immune cell association in mouse spleen revealed by immunofluorescent staining. *Sci Rep* 10;9850, 2020.

54. Giogrio, R, Sternini, C, Anderson, K, Brecha, N, Go, V: Tissue distribution and innervation pattern of peptide immunoreactivity in the rat pancreas. *Peptides* 1992, 13(1);91-98.

55. Ushiki, T, Watanabe, S: Distribution and ultra-structure of the autonomic verves in the mouse pancreas. *Microscop Res Tech* 1997, 37(5-6);399-406.

56. Rodriguez-Diaz, R, Caicedo, A: Novel approach to studying the role of innervation plays in the biology of pancreatic islets. *Endocrinol Metab Clin North Am* 2013, 42(1);39-56.

57. Chandra, R, Liddle, RA: Neural and hormonal regulation of pancreatic secretion. *Curr Oppin Gastroenterol* 2014, 30(5);490-494.

58. Tomita, T, Lacy, PE, Matschinsky, FM, McDaniel, M: Effects of alloxan on insulin secretion I isolated rat islets perifused in vitro. *Diabetes* 1974, 23(6);517-524.

59. Barthout, HR, Powley, TL: Identification of vagal preganglion that mediates cephalic phase insulin. *Am J Physiol* 1990, 258(2);R523-R530.

60. Li, W, Yu, G, Liu, Y, Sha, L: Intrapancreatic ganglia and neural regulation of pancreatic endocrine secretion. *Front Neurosci* 13;1-10,2019.

61. Ahren, B, Taborsky, GJJr: The mechanism of vagal nerve stimulation of glucagon and insulin secretion. *Endocrinol* 1986, 118(1);1551-1557.

62. Tomita, T, Friesen, SR, Kimmel, JR, Pollock, HG: Pancreatic polypeptide-secreting islet cell tumors. *Am J Pathol* 1983, 113 (2);134-142.

63. Mudler, J, Hokfelt, T, Knuepfer, MM, Kopp, UC: Renal sensory and sympathetic nerves re- innervate kidney in a similar time-dependent fashion after renal denervation in rats. *Am J Physiol Rregul Integr Physiol* 2013, 304(8);R675-R682.

64. Barajas, L, Powers, K: Monoaminergic innervation of rat kidney. A quantitative study. *Am J Physio* 259(pt2);F503-F511.

65. Mitchell, AGE: The nerve supply of the kidneys. *Acta Anat* 1950, 10(1);1-37.

66. Di Bona, GF, Kopp, UC: Nerve control of renal function. *Phys Rev* 1997, 77(1);75-197.

67. Ahren, B: Thyroid neuroendocrinology: Nerve regulation of thyroid hormone. *Endocr Rev* 1986, 7(2);149-155.

68. Amenta, F, Caporuscio, D, Ferrante, F, Porcelli, F, Zomparelli, M: Cholinergic nerves in the thyroid gland. *Cell Tissue Res* 1978, 195(2);367-370.

69. Grunditz, t, Hakenson, R, Rerup, C, Sundler, F, Uddman, R: Neuropeptide Y in the thyroid gland: neuronal localization and enhancement of stimulated thyroid hormone secretion. *Endocrinol* 115(4);1537-1542.

70. Silva, JE, Bianco, SD: Thyroid adrenergic interactions: Physiological and clinical implications. *Thyroid* 2008, 18(2);157-165.

71. Parker, TL, Kesse, WK, Mohamed, AA, Afework, M: The innervation of the mammalian adrenal gland. *J Anat* 1993, 183(pt 1);265-276.

72. Charlton, BG, Nkomazana, OF, Mc Gadey A, Neal, DE: A preliminary study of acetylcholine-esterase-positive innervation in the human adrenal cortex. *J Anat* 1991, 176;99-104.

73. Holgert, H, Gagerlind, A, Hokfelt, T: Immuno-histochemical characterization of epidermic innervation of the rat adrenal. *Horm Metab Res* 1998, 30(6-7);3156-3222.

74. Murabayashi, H, Kuramoto, H, Kawano, H, Sasaki, M, Katamura, N et al Immunohistochemical feature of substance p-immunoreactive chromaffin-cells and nerve fibers in the rat adrenal gland. *Arch Histol Cytol* 2007, 70(3);183-196.

75. Heym, C, Braun, B, Shuji, Y, Klimasschewski, L, Colombo-Benkmann, M: Immunohistochemical correlation of human adrenal verve fibers and thoracic dorsal root neurons with special reference to substance P. *Histochem Cell Biol* 1995, 104(3);233-243.

76. Fung, MM, Miveerros, OH, O'Conner, DT: Diseases of the adrenal medulla. *Acta Physiol* 2007, 192(2); 325-335.

77. Ji, RC, Kato, S: Intrinsic interrelationship of lymphatic endothelia with nerve elements in the monkey urinary bladder. *Acta Rec* 2000, 259(1);86-96.

78. Yoshimura, N, Chancellor, MB: Neurophysiology of the lower urinary tract function and dysfunction. *Rev Urol* 2003, 5(Suppl 8);s3-s10.

79. de Groat, W: Integrative control of the lower urinary tract: preclinical perspective. *Br J Pharmacol* 2006, 147(Suppl 2);s25-s40.

80. Andersson, KE: Bladder activation: afferent mechanisms. *Urol* 2002, 39(Suppl 1);43-50.

81. Bauer, MM, Smith, PG: Estrogen and female reproductive tract innervation: Cellular and molecular mechanisms of autonomic neuroplasticity. *Auton Neurosci* 2015, 187(1);1-17.

82. Hoyle, CV, Stones, RW, Robson, T, Whitley, K, Burnstock, GY: Innervation of vascular and microvasculature of the human vagina by NOS and neuropeptide-containing nerves. *J Anat* 1996, 188(3);633-644.

83. Li, T, Liau, H, Gao, X, Li, X et al: Anatomic distribution of nerves and microvascular density in the human anterior vaginal wall: Prospective study. *PLOS One*, 2014, 9(11):e110239.

84. Griebling, TL, Liao, Z, Smith, PG: Systemic and tropical hormone therapies reduce vaginal innervation density in postmenopausal women. *Menopause* 2012, 19(6);630-635.

85. Bae, SE, Corcoran, BM, Watson, DE: Immunohistochemical study of the distribution of adrenergic and peptidermic innervation in the equine uterus and the cervix. *Reproduction* 2001, 122 (2);275-282.

86. Spezio Sardo, D, Floria, A, Soss Fernandez, LM, Guerra, G, Spinelli, M et al: The potential role of endometrial nerve fibers in the pathogenesis of pain generation during endometrial biopsy at office hysteroscopy. *Reprod Sci* 2015, 22(1);124-131.

87. Donadio, V, Nolano, M, Porovitera, V, Stancanelli, A, Lullo, F et al: Skin sympathetic adrenergic innervation: an immunofluorescence confocal study. *Am Neurol* 2006, 59(2);376-381.

88. Lauria, G, Deviglia, G: Skin biopsy as a diagnostic tool in peripheral neuropathy. *Nat Clin Prac* 2007, 3(10);546-557.

89. Wang, N, Gibbons, CH, Freeman, R: Novel immunohistochemical technique using discrete signal amplification systems for human cutaneous peripheral nerve fiber imaging. *J Histochem Cytochem* 2011, 59(4);382-390.

90. Iwami, D, Ohi, R, Nio, M, Shimaoka, S, Sano, N: Abnormal distribution of nerve fibers in the liver of biliary atresia. *Tohoku J Exp Med* 1997, 181(1);57-65.

91. Akiyoshi, H, Gonad, T, Terada, T: A comparative histochemical and immunohistochemical study of aminergic, Cholinergic and peptidermic innervation in rat, hamster, guinea pig, dog and human liver. *Liver* 1998, 18(5);352-359.

92. Grant, WF, Nicol, L, Thorn, SR, Grove, KL, Friedman, JR et al: Peripheral exposure to a high-fat diet is associated with reduced hepatic sympathetic innervation in one-year male Japanese macaques. *PLOS One* 2012, 7(10):e48119.

93. Tomita, T: Localization of nerve fibers in colonic polyp, adenoma and adenocarcinoma by immunocytochemical staining for PGP 9.5. *Dig Dis Sci* 2012, 57(2);364-370.

94. Tomita, T: PGP 9.5 immunocytochemical staining for pancreatic endocrine tumors. *Islets* 2013, 5(1);1-7.